Supporting Information

Sustainable Hydrogen Peroxide Oxidation of Carboxylated Cellulose Nanocrystals: Efficient Modulation of Carboxyl Content, Hydrophilicity, and Particle Size for Tablet Formulation and Drug Release

Zilu Li[a], Xuefei Chen[a], Hou-Yong Yu[a,c]*, Chao Wu[a], Somia Yassin Hussain Abdalkarim[a], Yunfei Shen[c], Guojun Jin[b]*, Jia-Fu Zhu[d]

[a] *Key Laboratory of Intelligent Textile and Flexible Interconnection of Zhejiang Province, Zhejiang Sci-Tech University, Hangzhou 310018, China*

[b] *Department of Plastic Surgery, Linhai Branch, The Second Affiliated Hospital, Zhejiang University School of Medicine, Taizhou, Zhejiang, China*

[c] *Huzhou City Linghu Xinwang Chemical Co., Ltd, Huzhou 313018, China*

[d] *Department of Orthopaedics, Tongde Hospital of Zhejiang Province, Hangzhou 310012, People's Republic of China.*

*Corresponding authors. E-mail addresses: phdyu@zstu.edu.cn (Hou-Yong Yu), 19119025@sina.com (Guojun Jin), Phone: + 86-571-86843071

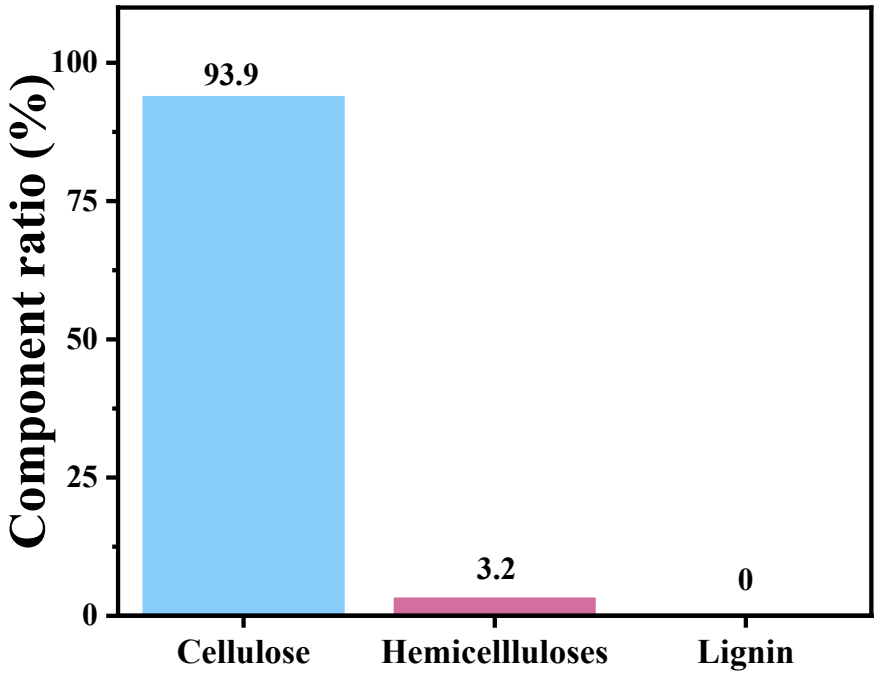

Fig. S1. Content of cellulose, hemicellulose, and lignin in microcrystalline cellulose

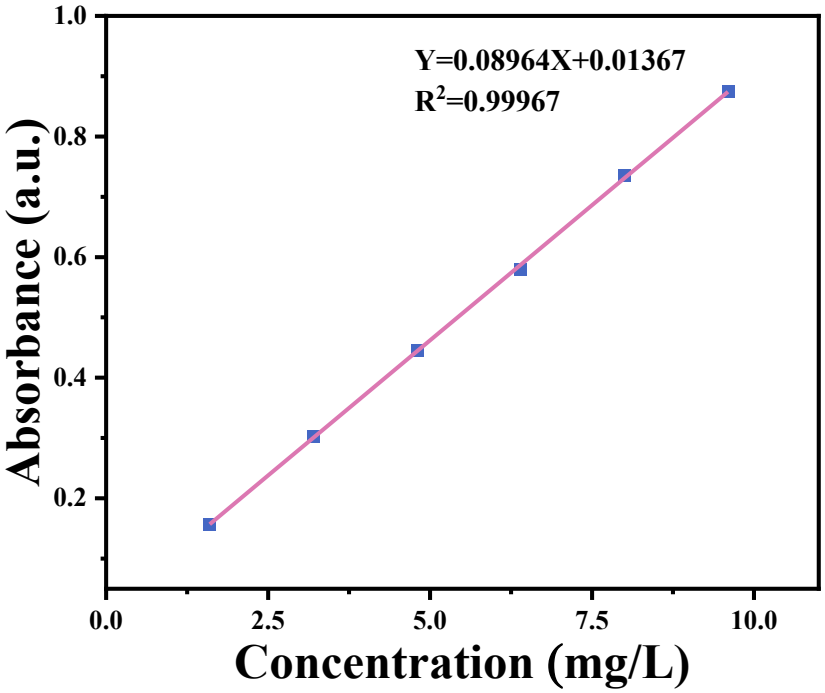

Fig. S2. Standard curve for UV absorbance of TCH.

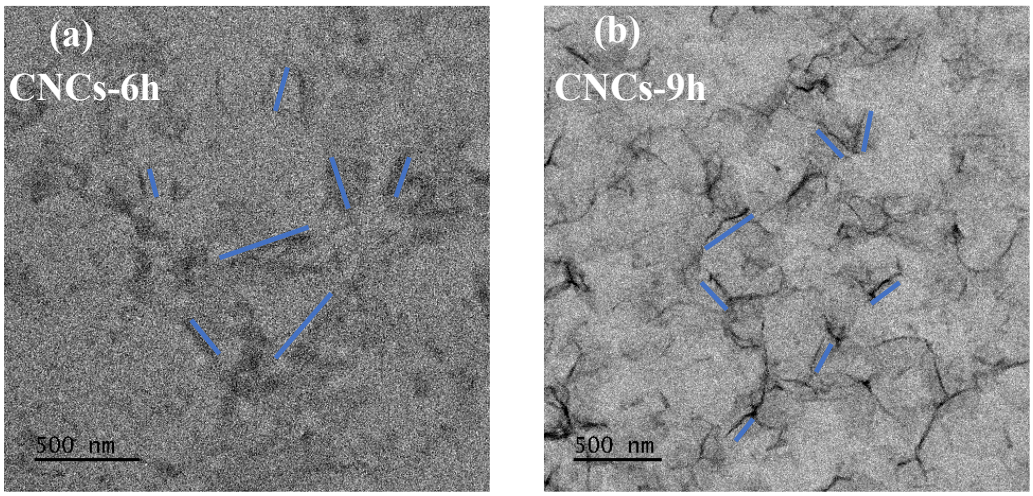

Fig. S3. TEM images of CNCs-6h (a), and CNCs-9h (b).

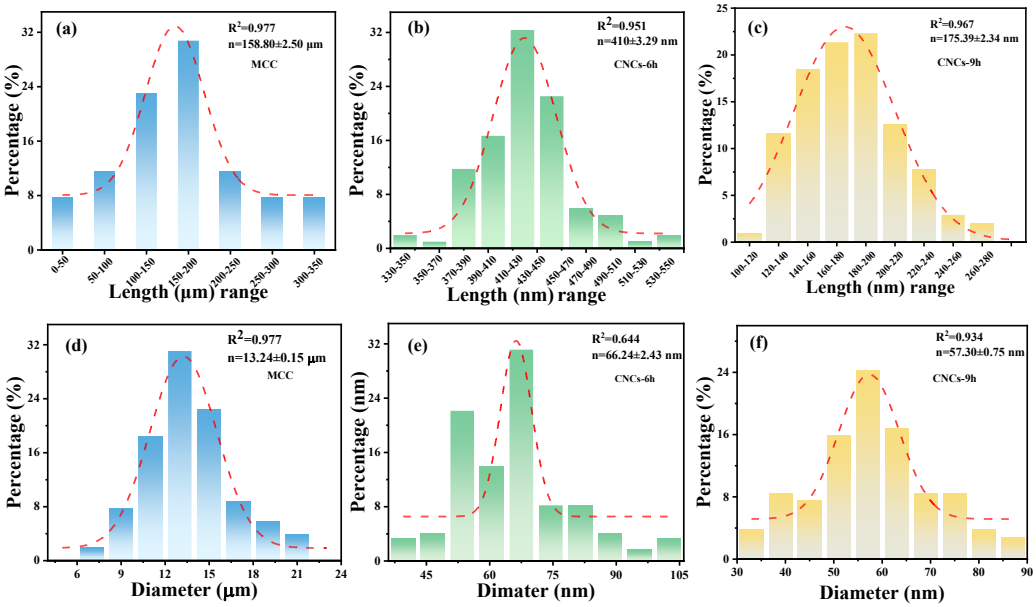

Fig. S4. Average geometrical length range and width of MCC (a, d), CNCs-6h (b, e), and CNCs-9h (c, f)

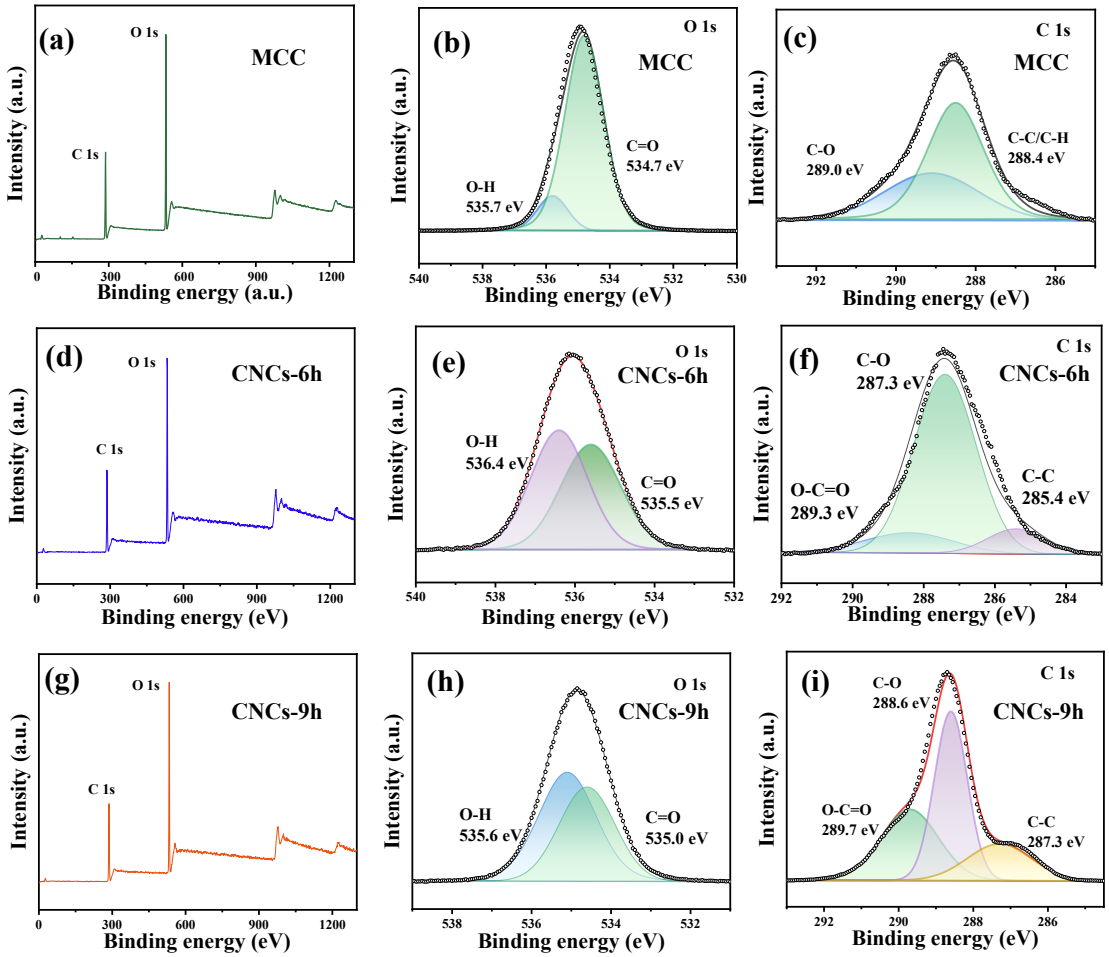

Fig. S5 XPS survey spectra for MCC (a-c), CNCs-6h(d-f), and CNCs-9h(g-i)

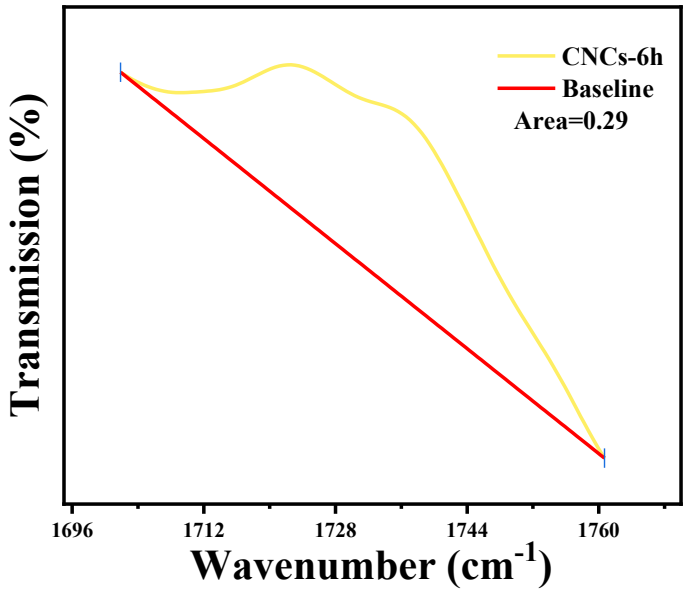

Fig. S6. Carboxy peak area of CNCs-6h

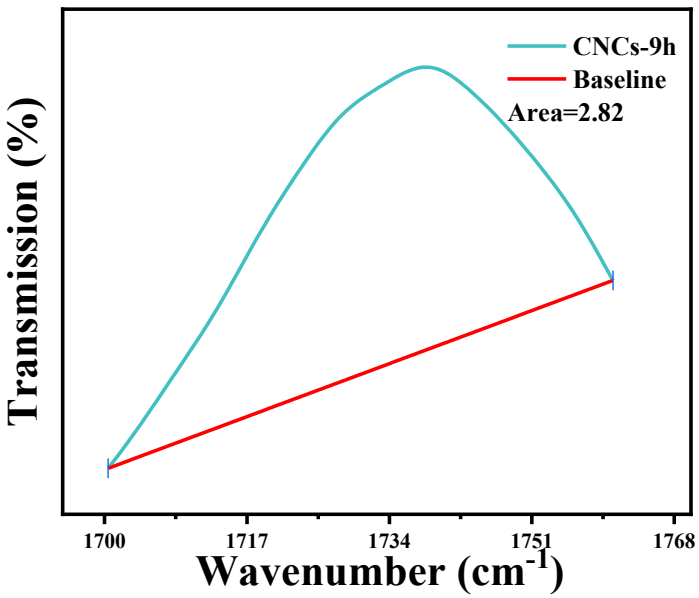

Fig. S7. Carboxy peak area of CNCs-9h

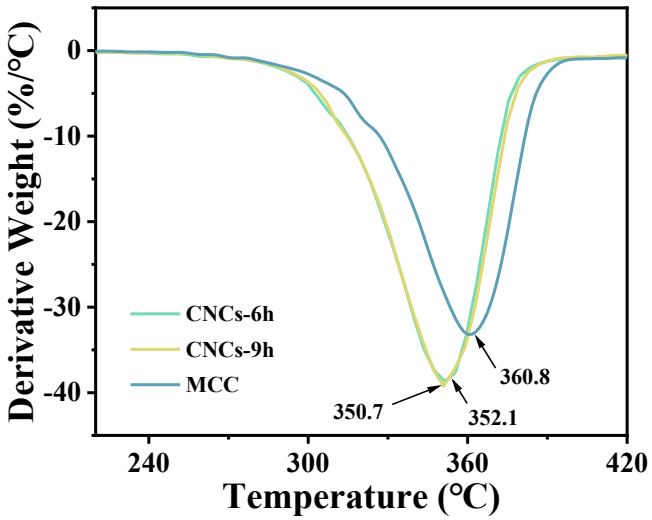

Fig. S8. DTG curves of MCC, CNCs-6h, and CNCs-9h.

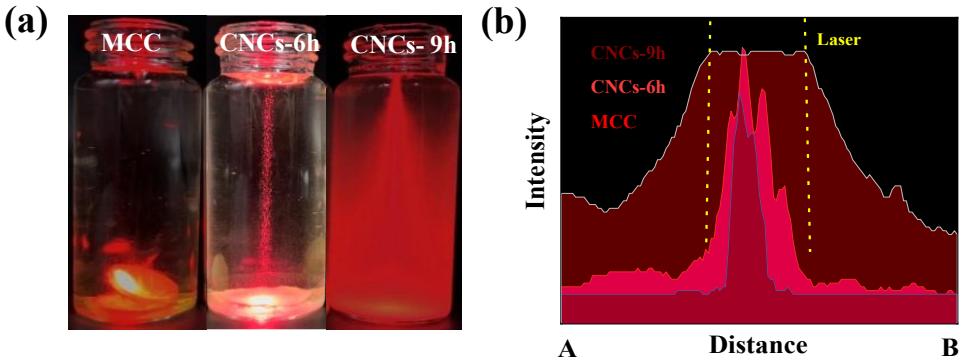

Fig. S9. (a)Release behavior of pharmaceutical excipient tablets after 240s of laser irradiation in water. (b) Relationship between light intensity and the distance from panel A to B.

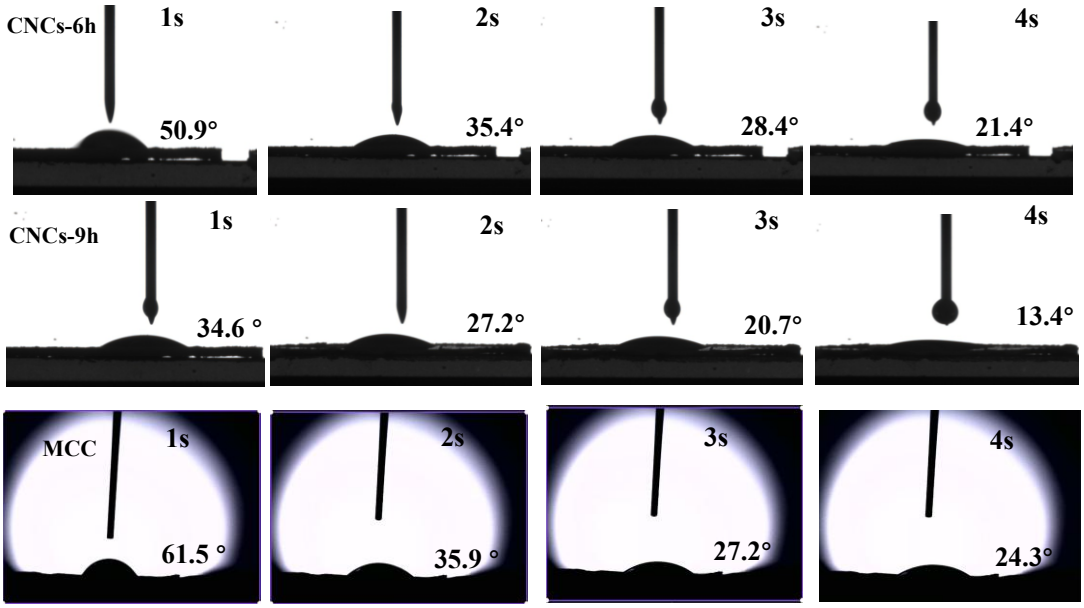

Fig. S10. Dynamic water contact angle testing of MCC, CNCs-6h, and CNCs-9h

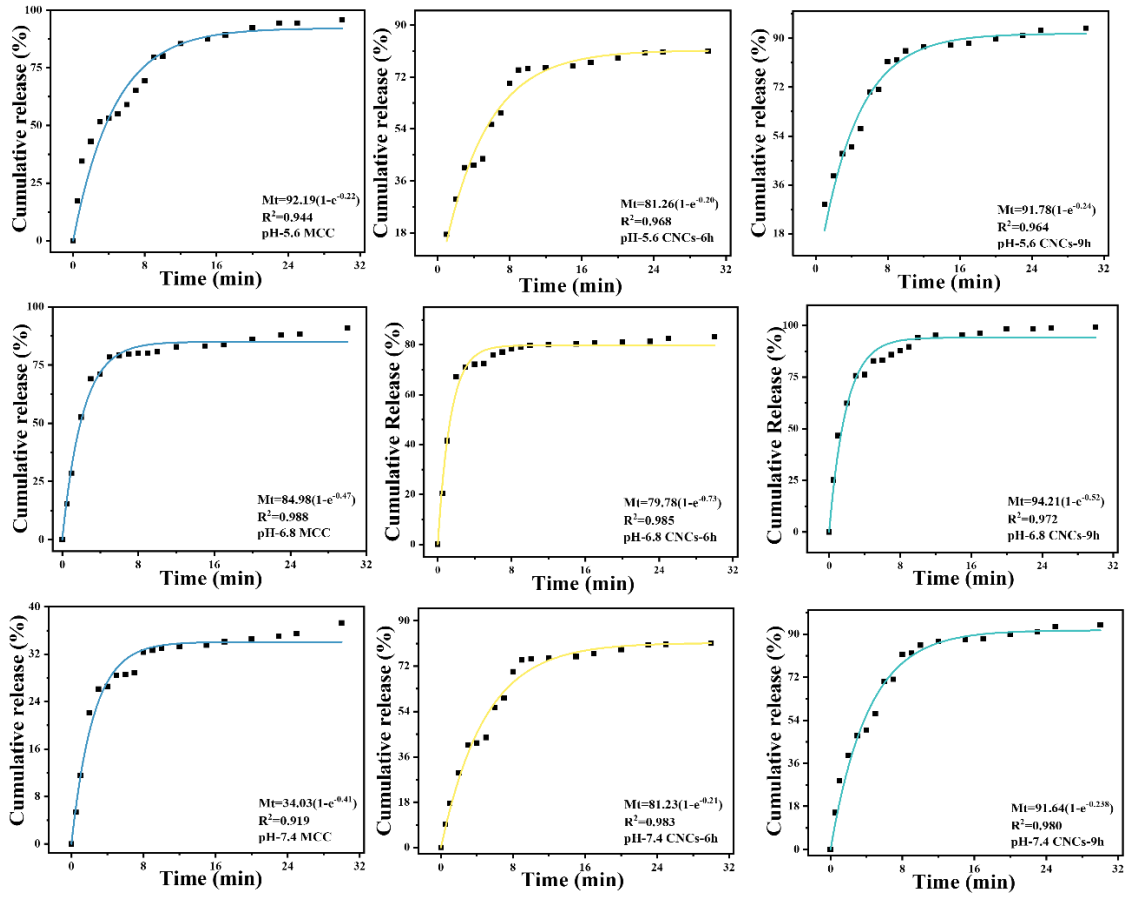

Fig. S11. First-order kinetic fitting of drug release from direct compression cellulose tablets.

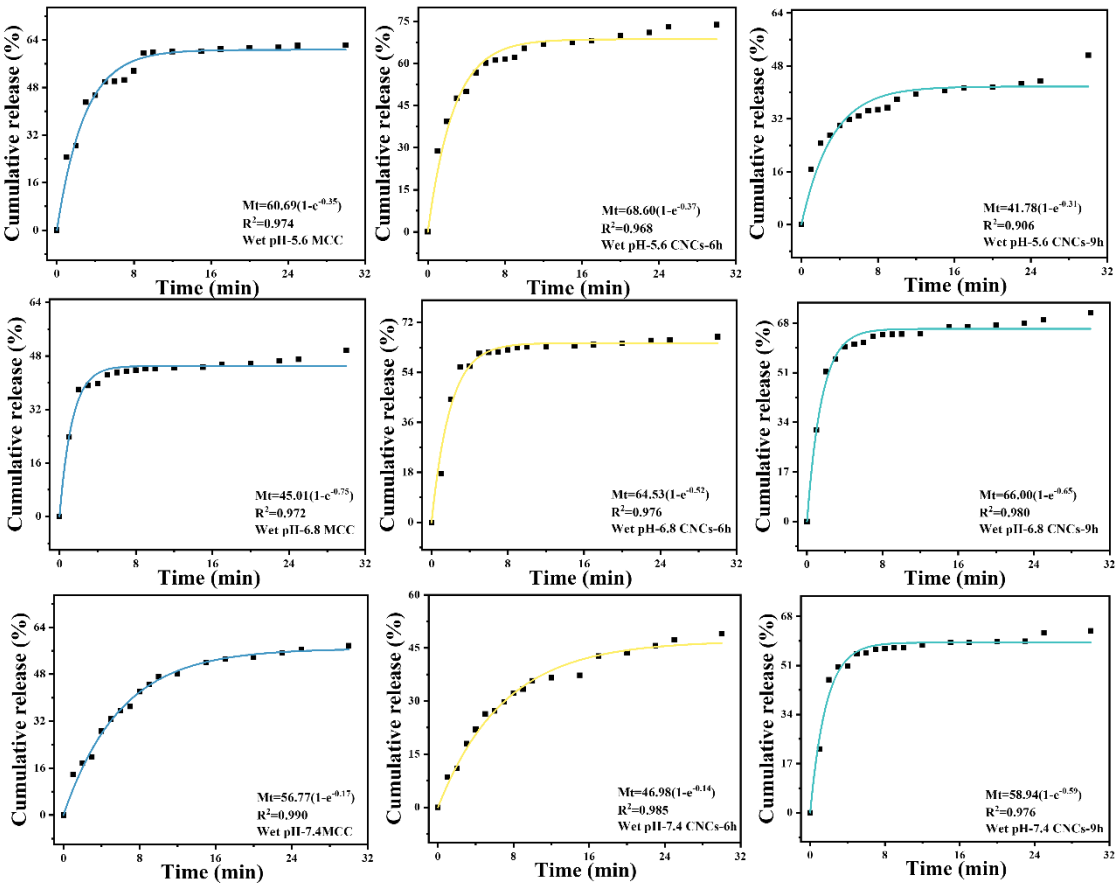

Fig. S12. First-order kinetic fitting of drug release from wet granulated cellulose tablets.

Table S1. Comparative study of the properties of cellulose nanocrystals prepared by different methods

Sample	Diameter (nm)	Length (nm)	Crystallinity (%)	Zeta Potential (mV)	Carboxyl Content (mmol/g)	T_0(℃)	T_{max}(℃)	Surface Functional Groups	Ref.
CNCs-6h	66.24±2.43	410.00±3.29	80.92 ± 1.19	-18.9±1.17	0.8 ± 0.08	324.9	352.1	$-COO^-$	This work
CNCs-9h	57.30±0.75	175.39±2.34	82.53 ± 0.67	-23.5±0.86	1.2 ± 0.11	318.6	350.7	$-COO^-$	This work
CNC-acid-sulfate	23.0±8.9	169.9±86.8	88.6	-40.4±1.7	/	250-260	330	$-OSO_3^-$	[1]
CNC-TEMPO oxidation	3-10	110-200	40	/	1.2-1.7	/	200-300	$-COO^-$	[2]
CNC-H_2O_2 Oxidation	23	263	77.5	-20.8	1.0	/	/	$-COO^-$	[3]
Commerical CNC	20-30	250-450	67	90-123	0.65	207.3	/	$-COO^-$	[4]

66 **Table S2.** Mobility evaluation based on compressibility and the Hausner ratio

Compression ratio (%)	Shifting	Hausner ratio
≤ 10	rare	1.00-1.11
11-15	good	1.12-1.18
16-20	Better	1.19-1.25
21-25	general	1.26-1.34
36-31	poor	1.35-1.45
32-37	Very poor	1.46-1.59
> 38	Extremely poor	> 1.60

67 **Table S3.** MCC, CNCs-6h, CNCs-9h compressibility and Hausner ratio

Sample	Compression ratio (%)	Hausner ratio
MCC	6.67	1.07
CNCs-6h	23.45	1.32
CNCs-9h	12.56	1.17

68

Table S4. Residual iron content in CNC determined by ICP-OES

Sample	Sample mass m_0 (g)	Final volume V_0 (mL)	Element	Measured concentration C_0 (mg·L^{-1})	LOD (mg·L^{-1})	Dilution factor f	Digested solution concentration C_1 (mg·L^{-1})	Element content C_x (mg·kg^{-1})	Mean ± SD (mg·kg^{-1})
CNCs-6h-1	**0.05185**	**50**	**Fe**	**0.0233**	**＜0.01**	**1**	**0.02330**	**22.47**	**23.5**
CNCs-6h-2	**0.05143**	**50**	**Fe**	**0.0252**	**＜0.01**	**1**	**0.02520**	**24.50**	**23.5**
CNCs-9h-1	**0.05180**	**50**	**Fe**	**0.0239**	**＜0.01**	**1**	**0.02390**	**23.07**	**22.6**
CNCs-9h-2	**0.05237**	**50**	**Fe**	**0.0231**	**＜0.01**	**1**	**0.02310**	**22.05**	**22.6**

Table S5. Carboxyl group content of CNCs-6h and CNCs-9h determined by conductometric titration

Sample	Replicate 1	Replicate 2	Replicate 3	Carboxyl content (mmol/g)
CNCs-6h	0.8	1.0	0.7	0.83 ± 0.15
CNCs-9h	1.1	1.3	1.4	1.27 ± 0.15

Table S6. Zeta potential multiple measurements with mean, standard deviation, and standard error.

Sample (mV)	Test 1	Test 2	Test 3	Test 4	Test 5	Test 6	$\bar{x}$	(SD)	(SE)
MCC	-13.6	-11.6	-12.9	-11.7	-13.8	-12.6	-12.7	0.93	0.38
CNCs-6h	-19.8	-16.7	-18.5	-19.8	-18.9	-19.7	-18.9	1.17	0.48
CNCs-9h	-24.5	-23.6	-22.1	-23.2	-23.3	-24.3	-23.5	0.86	0.35

Table S7. Crystallinity index of MCC, CNCs-6h and CNCs-9h (mean ± SD, n = 3)

Sample	CrI (%) – Replicate 1	CrI (%) – Replicate 2	CrI (%) – Replicate 3	CrI (Mean ± SD)
MCC	73.98	75.42	76.95	75.45± 1.52
CNCs-6h	79.85	80.96	81.95	80.92 ± 1.19
CNCs-9h	81.88	82.54	83.17	82.53 ± 0.67

77

78 **Table S8.** BET specific surface area of MCC, CNCs-6h and CNCs-9h (mean ± SD, n = 3)

Sample	BET surface area (m^2/g) 1	BET surface area (m^2/g) 2	BET surface area (m^2/g) 3	BET surface area (m^2/g) (Mean ± SD)
MCC	0.48	0.52	0.56	0.52±0.04
CNCs-6h	3.18	3.27	3.36	3.27±0.09
CNCs-9h	6.17	6.32	6.41	6.32±0.15

79

80

81 **Table S9. Hardness, friability, disintegration time, and mass of tablets**

Sample	Tablet mass (mg, n=10, mean ± SD)	Friability (%, n=10, mean ± SD)	Static disintegration time (s, n=6, mean ± SD)	Dynamic disintegration time (s, n=6, mean ± SD)	Hardness (N, n=6, mean ± SD)
DM	1428.1±23.6	1.23±0.05	240 ± 5	90±3	54.3± 0.8
DC-6	1452.5±24.7	0.43±0.04	80 ± 4	15±4	72.6± 2.3
DC-9	1432.5±30.4	0.07±0.01	10 ± 3	3±1	75.3± 1.7
WM	1250.5±34.6	0.98±0.05	240±10	120±10	60.8± 2.1
WC-6	1220.5±92.6	0.36±0.03	100±8	30±5	80.5± 1.6
WC-9	1286.0±15.5	0.14±0.01	60±5	10±2	90.2± 2.9

Table S10 Roughness of CNCs-6h and CNCs-9h

Sample	Sq(μm)	Sa(μm)	Sp(μm)	Sv(μm)	Sz(μm)	Ssk	Sku
CNCs-6h	0.0049	0.004	0.0256	0.0114	0.037	0.6458	3.0639
CNCs-9h	0.004	0.0032	0.0199	0.009	0.0288	1.0632	3.8206

Table S11. Yield and structural characteristics of CNCs-9 h, NCC, and CNF

Sample	Yield (%)	Diameter(nm)	Length(nm)	Crystallinity (%)	Ref
CNCs-9h	91.4	30-90	100-300	85.4	This work
CNF	30.2	5-20	500-2000	65.2	[5-7]
NCC	45.6	10-20	200–500	72.4	[8]

Table S12. TCH releases kinetic fitting results of direct compression.

pH-5.6	**Sample**	**MCC**			**CNCs-6h**			**CNCs-9h**		
Direct Model	**Formula**	**K**	**n**	**R^2**	**K**	**n**	**R^2**	**K**	**n**	**R^2**
Zero-order	$\frac{M_t}{M_\infty} = Kt$	2.634	/	0.711	1.589	/	0.758	1.726	/	0.556
First-order	$Ln\left(1 - \frac{M_t}{M_\infty}\right) = Kt$	0.221	/	0.944	0.201	/	0.968	0.237	/	0.962
Higuchi	$\frac{M_t}{M_\infty} = Kt^{\frac{1}{2}}$	5.268	/	0.711	3.453	/	0.556	3.177	/	0.758
Ritger-Peppas	$\frac{M_t}{M_\infty} = Kt^n$	35.025	0.322	0.615	28.638	0.283	0.678	18.384	0.350	0.776

Table S13. TCH releases kinetic fitting results of wet granulation.

pH-5.6	Sample	MCC			CNCs-6h			CNCs-9h		
Wet Model	**Formula**	**K**	**n**	**R^2**	**K**	**n**	**R^2**	**K**	**n**	**R^2**
Zero-order	$\frac{M_t}{M_\infty} = Kt$	1.723	/	0.545	1.087	/	0.336	1.066	/	0.650
First-order	$Ln\left(1 - \frac{M_t}{M_\infty}\right) = Kt$	0.348	/	0.974	0.372	/	0.968	0.312	/	0.906
Higuchi	$\frac{M_t}{M_\infty} = Kt^{\frac{1}{2}}$	3.445	/	0.545	3.027	/	0.508	2.133	/	0.650
Ritger-Peppas	$\frac{M_t}{M_\infty} = Kt^n$	34.656	0.245	0.721	29.737	0.252	0.698	20.450	0.252	0.752

Table S14. Comparison of cellulosic materials as pharmaceutical excipients in different relevant studies.

104

Sample	Preparation method	Yield (%)	Drug type	Drug release rate (%)	Pressing method	Disintegration rate (s)	Friability (%)	Ref.
Cellulose Nanocrystal Membranes	Acid hydrolysis	14.15	tablet	10	/	/	/	9
Cellulose nanocrystals	Sulfuric acid hydrolysis	76	Oral dispersible tablets	/	Direct Compression	>10	/	10
Microcrystalline Cellulose	acid/base treatment	/	tablet	80	Direct Compression	90	0.15	11
nanocellulose	sulfuric acid	88	tablet	81.2	/	7	/	12
cellulose nanowhiskers	sulfuric acid hydrolysis	/	tablet	92	/	/	/	13
Sugarcane bagasse microcrystalline cellulose	sulfuric acid hydrolysis	29.9	tablet	66	Direct compression	339.83	/	14

Cellulose nanocrystals	**Hydrogen peroxide hydrolysis**	**91.4**	**tablet**	**96.8**	**Direct compression vs. Wet granulation**	**10**	**0.07**	**This work**

105

106

107

Video 1. Tablet Preparation Process

Characterization

The yield of CNCs was calculated using the Shweta[14] method. The morphology and elemental distribution of cellulose were observed by a field emission scanning electron microscope (FE–SEM, JM-5610, JEOL, Japan) at room temperature with an accelerating voltage of 3.00 kV. The chemical structure was detected by a Nicolet IS50 Fourier transform infrared spectrometer (FT-IR) at a resolution of 2 cm^{-1} in the wavelength range of 4000-400 cm^{-1}. The particle size and zeta potential of CNCs and MCC were determined in a Nano ZS Malvern Zetasizer. Thermal stability was assessed using a thermogravimetric analyzer (TG209 F1, Netzsch) in a dynamic nitrogen atmosphere at a gas flow rate of 30 mL/min, and TGA curves were recorded at a rate of 20 °C /min over the temperature range of 30 °C to 600 °C. X-ray diffraction tests (XRD; ARL X'TRA, Thermo Electron Corp) were performed using Cu Kα (1.5418 Å) rays (40 kV, 40 mA). The crystallinity (CrI) of MCCs and CNCs was calculated by the Yu method. Data Physics OCA40 contact angle analyzer was used for water contact angle testing of MCC and CNCs. MCC and CNCs were added to 500 mL of water, respectively, stirred, and mixed for a while. The liquid portion of the MCC and CNCs was separated using a pumping bottle and a Brinell's funnel, and the filtered powdered samples of MCC and CNCs were placed in a constant temperature oven for drying. The mass of the samples before and after drying was recorded, and the water content was calculated. The excipients and active pharmaceutical ingredients were uniformly mixed using a mixer (VH5; Shanghai Tian Helu Machinery Equipment Co.) at a rotational speed of 24 r/min. The specific surface areas of MCC and CNC were determined by the Brunauer-Emmet-Teller method (Mack Instruments, ASAP2020 gas adsorption system, USA).

References

1. N. Lin and A. J. N. Dufresne, *Nanoscale,* 2014, **6**, 5384-5393.
2. G. Kwon, K. Lee, D. Kim, Y. Jeon, U.-J. Kim and J. J. You, *Journal of Hazardous Materials,* 2020, **398**, 123100.
3. X.-M. Fan, H.-Y. Yu, D.-C. Wang, Z.-H. Mao, J. Yao, K. C. J. Tam and Engineering, *ACS Sustainable Chemistry & Engineering,* 2019, **7**, 18067-18075.
4. R. Koshani, T. G. van de Ven, A. J. Madadlou, *Journal of Agricultural and Food Chemistry,* 2018, **66**, 7692-7700.
5. J. Xu, E. F. Krietemeyer, V. M. Boddu, S. X. Liu and W.-C. J. Liu, *Carbohydrate Polymers,* 2018, **192**, 202-207.
6. K. Löbmann and A. J. J. Svagan, *International Journal of Pharmaceutics,* 2017, **533**, 285-297.
7. B. Yang, M. Zhang, Z. Lu, J. Tan, J. Luo, S. Song, X. Ding, L. Wang, P. Lu, and Q. J. *Carbohydrate Polymers,* Zhang, 2019, **208**, 372-381.
8. R. D. Gupta and N. J. Raghav, *International Journal of Biological Macromolecules,* 2020, **147**, 921-930.
9. A. Barbosa, E. Robles, J. Ribeiro, R. Lund, N. Carreño, and J. Labidi, *Materials*, 2016, **9**.
10. S. L. Almeida, R. L. Lazo, J. Carneiro, A. Caldonazo, C. Pires, I. F. Andreazza, and F. S. Murakami, *Journal of Drug Delivery Science and Technology*, 2024, **96**.
11. C. Viera-Herrera, J. Santamaría-Aguirre, K. Vizuete, A. Debut, D. C. Whitehead and F. Alexis, *Nanomaterials*, 2020, **10**.
12. X. Li, D. Ye, Z. Xiang, H. Wang, H. Wang, Y. Lu, and R. Yao, *Industrial Crops and Products*, 2023, **197**.
13. J. C. O. Villanova, E. Ayres, S. M. Carvalho, P. S. Patrício, F. V. Pereira and R. L. Oréfice, *European Journal of Pharmaceutical Sciences*, 2011, **42**, 406-415.
14. S. Mishra, *ACS Omega*, 2024, **9**, 19353-19362.